fermentation

MDPI

Article

Enhancing Nutritional Value and Sensory Quality of Spirulina (*Arthrospira platensis*) Through Preharvest Co-Cultivation with Yeast *Saccharomyces cerevisiae*

Yue Zhao [1,2], Jikang Sui [1,2], Yuxuan Cui [1,2], Mingyong Zeng [1,2,*], Haohao Wu [1,2,3,*], Guangxin Feng [1,2] and Xiangning Lu [4]

[1] State Key Laboratory of Marine Food Processing & Safety Control, College of Food Science and Engineering, Ocean University of China, Qingdao 266404, China; zhaoy021@163.com (Y.Z.); suijk_ouc@163.com (J.S.); 18846061783@163.com (Y.C.); fgxscut@163.com (G.F.)
[2] State Key Laboratory of Marine Food Processing & Safety Control, Sanya Oceanographic Institution, Ocean University of China, Sanya 572022, China
[3] Laoshan Laboratory, Qingdao 266000, China
[4] College of Marine Sciences, Ningbo University, Ningbo 315000, China; xiangninglu@foxmail.com
* Correspondence: mingyz@ouc.edu.cn (M.Z.); wuhaohao@ouc.edu.cn (H.W.); Tel.: +86-532-6089-2400 (M.Z.)

Abstract

Spirulina's (*Arthrospira platensis*) use in food applications is limited by its dark color and sulfurous odor. This study aimed to develop a preharvest bioprocessing strategy using *Saccharomyces cerevisiae* co-cultivation to address these limitations. At a yeast/microalgae biomass ratio of 10:1000 with 5 g/L of glucose supplementation, co-cultivation for 24 h induced a rapid color transition from dark blue–green to light green and imparted "floral–fruity" aromas. Major bioactive compounds, including β-carotene, linoleic acid, and γ-linolenic acid, increased significantly, while volatile sulfur compounds were eliminated. Chlorophyll a and carotenoid contents rose by over two fold, reflecting enhanced photosynthetic efficiency. Mechanistic analyses revealed that yeast-derived acetic acid upregulated genes involved in flavor precursor biosynthesis and promoted biomass accumulation. This strategy integrates sensory improvement with nutritional enhancement, providing a sustainable approach for developing spirulina-based functional foods.

Keywords: co-cultivation; nutritional value; spirulina; yeast; sensory quality

check for updates

Academic Editor: Giacomo Zara

Received: 9 July 2025
Revised: 4 August 2025
Accepted: 9 August 2025
Published: 11 August 2025

Citation: Zhao, Y.; Sui, J.; Cui, Y.; Zeng, M.; Wu, H.; Feng, G.; Lu, X. Enhancing Nutritional Value and Sensory Quality of Spirulina (*Arthrospira platensis*) Through Preharvest Co-Cultivation with Yeast *Saccharomyces cerevisiae*. *Fermentation* **2025**, *11*, 462. https://doi.org/10.3390/fermentation11080462

Copyright: © 2025 by the authors. Licensee MDPI, Basel, Switzerland. This article is an open access article distributed under the terms and conditions of the Creative Commons Attribution (CC BY) license (https://creativecommons.org/licenses/by/4.0/).

1. Introduction

Under the global carbon neutrality initiative, the development of novel food products that combine sustainability with nutritional benefits has emerged as a critical research focus in food science. Recognized by the FAO as a "future superfood", spirulina (*Arthrospira platensis* and *Arthrospira maxima*) has attracted significant attention due to its rich content of high-quality protein (60–70%), polyunsaturated fatty acids including γ-linolenic acid, and natural pigments such as phycocyanin and β-carotene, all demonstrating important functional nutritional properties [1]. However, spirulina can hardly be incorporated into commercial foods in large quantities due to its undesirable dark blue–green color and seaweed/muddy odor. Currently most research on sensory quality improvement of spirulina biomass is focused on postharvest processing technologies, e.g., microencapsulation, fermentation, and masking.

Microalgae–microbial symbiosis is a common natural phenomenon that shapes the diversity and structure of aquatic ecosystems [2]. There is increasing interest in leveraging

photoautotroph–heterotroph associations to enhance microalgae biomanufacturing [3]. Yeast is a particularly appealing edible microorganism with the potential to serve as a photoautotrophic partner due to its lack of endotoxins, high growth rate, and robustness to withstand alkaline pH levels [4]. Yeast can establish an obligatory symbiotic relationship with microalgae in co-culture systems by mutually benefiting each other through the exchange of metabolites (e.g., O_2, CO_2, and organic acids) [5,6]. The microalgae–yeast co-culture systems have been explored for applications in biodiesel production, wastewater treatment, chemical production, and aquaculture feed supply [7]. Co-culture strategies have been demonstrated to increase the yields of microalgae pigments and beneficial components/flavor precursors (e.g., lipids and carotenoids) [8,9]. Therefore, microalgae–yeast co-culture is a potential alternative strategy for improving the nutritional value and sensory quality of spirulina biomass at the preharvest stage.

Saccharomyces cerevisiae is a species of yeast instrumental in food processing (e.g., brewing, baking, and winemaking) and has been categorized as a Generally Recognized as Safe (GRAS) microorganism by the US Food and Drug Administration. However, there are few examples of co-cultivation of spirulina and *S. cerevisiae*. The present study established an efficient co-culture system comprising *A. platensis* and *S. cerevisiae* and compared color appearance, bioactive compound composition, aroma quality, and volatile flavor profile between monocultured and co-cultured *A. platensis* to assess nutritional and sensory acceptability as a future food. In addition, the plentiful organic acids generated by *S. cerevisiae* in alkaline medium were shown to be responsible for the stimulated β-carotene, linoleic acid, and γ-linolenic acid biosynthesis in co-cultured *A. platensis*.

2. Materials and Methods

2.1. Microorganism Strains and Pre-Culture Conditions

A. platensis (FACHB-902) was purchased from the Freshwater Algae Culture Collection at the Institute of Hydrobiology (FACHB), Chinese Academy of Sciences (Wuhan, China). Arthrospira remains the taxonomically validated classification per phylogenomic evidence (current study), whereas Limnospira remains a contentious proposal lacking consensus. Before co-culture experiments, *A. platensis* was cultured to the late-logarithmic phase in Zarrouk medium (Tables S1 and S2) in 5 L reactors. The 0.45 μm filtered compressed air was introduced at the bottom of the column to supply carbon and prevent cell aggregation.

S. cerevisiae CICC 1251 was obtained from the China Center of Industrial Culture Collection (CICC). Before co-culture experiments, *S. cerevisiae* was cultured in Yeast Extract Peptone Dextrose Agar (YPDA) at 28 °C for 48 h to the logarithmic phase, transferred to Zarrouk medium at a final concentration of 6−7 log CFU/mL, stored at 4 °C, and used within 12 h.

2.2. Co-Culture Experiments

The resuspension of *S. cerevisiae* was added to the logarithmic growth phase of *A. platensis* and co-cultivated in 5 L Zarrouk medium supplemented with 5 g/L glucose. The late-logarithmic phase pre-culture of *A. platensis* at the OD_{560} of 0.8 ± 0.05 was inoculated with *S. cerevisiae* at yeast-to-microalgae biomass ratios of 1:1000, 10:1000, and 100:1000. During the co-cultivation, the co-cultures were kept in a constant-temperature oscillation incubator at 30 ± 5 °C under a light intensity of 100 μmol photons·$m^{-2}s^{-1}$. The 0.45 μm filtered compressed air was introduced at the bottom of the column to supply carbon and prevent cell aggregation. All experiments were performed at least in triplicate.

Biomass was estimated by OD_{560}, direct cell counting, and the dry weight method. Throughout the cultivation phase, the OD_{560} of a culture aliquot was measured using a UV-Vis spectrophotometer (Shimadzu, Kyoto, Japan). Cell counting was performed using

a dilution series with a hemocytometer and an optical microscope (Nikon Ts2 FL, Nikon, Tokyo, Japan). To measure dry weight, a certain volume of culture aliquot (V) was filtered through a 0.45 μm Whatman GF/C glass-fiber filter, and after the filter paper was oven-dried, the dry weight was measured by subtracting the weight of the original filter paper (M1) from the weight of the paper after cell filtration (M2). The biomass concentration (g/L) was calculated using the following equation [10]:

$$\text{Biomass concentration}(\text{g/L}) = \frac{M_2 - M_1}{V} \quad (1)$$

Dissolved oxygen values were estimated using a JPBJ-610L DO meter (INESA Scientific Instrument, Shanghai, China).

2.3. Profiling of Yeast Extracellular Organic Acids

S. cerevisiae was cultured in Zarrouk medium supplemented with 5 g/L glucose at 30 °C for 36 h, followed by centrifugation at 6000× *g* for 10 min at 4 °C. The supernatant was then filtered and collected as the yeast culture supernatant, which was lyophilized for the profiling of organic acids. Organic acids were analyzed as previously reported with minor modifications [11]. Briefly, 0.9 g of the sample was mixed with 10 mL of ultrapure water with ultrasonic treatment for 30 min. The supernatant was filtered through a 0.22 μm filter and analyzed using an HPLC system (Agilent Series 1260, Agilent Technologies, Santa Clara, CA, USA) equipped with an Agilent C18 AQ analytical column (4.6 mm × 250 mm, 5 μm). Organic acids were quantified based on retention times and area of the standard mixture of the following 9 organic acids: oxalic acid, tartaric acid, malic acid, lactic acid, acetic acid, maleic acid, citric acid, succinic acid, and fumaric acid. A methanol-buffered salt solution (5:95, *v*/*v*) was used as the mobile phase with a flow rate of 1.0 mL/min.

2.4. Color Evaluation and Pigment Analysis

Microalgae cells were harvested at 24 h post-yeast inoculation for color evaluation and pigment analysis. The chromatism measurements of lyophilized microalgae powders were performed using a CR-400 colorimeter (Konica Minolta, Tokyo, Japan) equipped with a Commission Internationale de l'Éclairage (CIE) color system. The results are presented as *L** (brightness), *a** (+a, red; −a, green), and *b** (+b, yellow; −b, blue).

The contents of Chlorophyll a (Chl. a) and carotenoids in *A. platensis* biomass were determined as previously described with some modifications [12]. Briefly, the microalgae were extracted using an 80% acetone solution (*v*/*v*) at 4 °C until almost colorless. The extract was then measured at wavelengths of 670 nm, 646 nm, and 470 nm. The concentrations of the pigments were calculated using the following equations:

$$\Delta A = A_{\text{test}} - A_{\text{blank}} \quad (2)$$

$$C_{Chl.\ a}\ (\text{mg/L}) = 12.25 \times \Delta A_{663} - 2.79 \times \Delta A_{646} \quad (3)$$

$$C_{carotenoids}\ (\text{mg/L}) = 5.05 \times \Delta A_{470} - 0.009 \times C_{Chl.\ a} - 9.22 \times \Delta A_{646} + 2.19 \times \Delta A_{663} \quad (4)$$

Carotenoids in *A. platensis* biomass were profiled based on HPLC analysis as previously described [13]. Briefly, lyophilized microalgae samples were ground at 4 °C for 10 cycles of 60 s using a tissue grinding machine (Servicebio, Wuhan, China); this was followed by repeated extraction with methyl tertiary butyl ether until the biomass was almost colorless. After centrifugation at 6000× *g* for 10 min, the extract was dried with nitrogen gas, reconstituted in 500 μL of acetone, filtered through a 0.22 μm filter, and analyzed on an HPLC system equipped with a ZORBAX Eclipse XDB-C18 reverse phase column (4.6 mm × 250 mm, 5 μm; Agilent, USA).

2.5. Sensory and Instrumental Volatile Flavor Analysis

Microalgae cells were harvested 24 h post-yeast inoculation for sensory and instrumental volatile flavor analysis. Sensory evaluation of volatile flavor was conducted in a standardized sensory booth (ISO 8589) under controlled lighting and ventilation conditions [14]. The evaluation was performed by a team of panelists consisting of 8 males and 7 females, who were graduate students or faculty members from several different labs and were trained and selected according to the guidelines in ISO 5496, ISO 8586, and GB/T 39625 (China National Standard) [15–19]. These panelists had correction rates >80% in odor tests. Lyophilized microalgae samples (2 g) were kept in odorless clear SPME vials for 30 min at room temperature before being sniffed by the panelists. The free choice profiling (FCP) method was employed to generate an odor vocabulary. Sensory scores, ranging from 0 to 10, were assigned to microalgae samples based on the odor intensity.

The volatile compounds were characterized through headspace solid-phase microextraction (SPME) coupled with gas chromatography–mass spectrometry (GC-MS) as previously described [20]. To facilitate the volatilization of odorants, a saturated NaCl solution (~26%) was used to prepare the microalgae suspension (40 g/L), 2 mL of which was then transferred to a 20 mL SPME glass vial, and 20 µL of 2-methyl-3-heptanone (100 µg/g) was added as an internal standard. After a 20 min incubation at 60 °C with agitation at 300 rpm, the extraction needle (50/30 µm, DVB/CAR/PDMS 57348-U; Supelco, Bellefonte, PA, USA) was inserted for a 30 min headspace extraction of volatile compounds, followed by heating at 250 °C at the gas-injection port for 20 min. The volatile compounds were analyzed using an Agilent 7890A-5975C GC-MS system (Agilent, USA) equipped with an INNOWAX column (60 m × 0.25 mm, 0.25 µm; Agilent, USA). The carrier gas, helium, was injected at a flow rate of 1.2 mL/min. The temperature program was set as follows: 40 °C, holding for 5 min, ramping to 240 °C at a rate of 5 °C/min, ramping to 250 °C at a rate of 10 °C/min, and holding for 6 min. The mass scan range was set at 29–550 Da, and the electron energy was set at 70 eV. Three replicates were used for each microalgae sample in the SPME-GC-MS analysis.

2.6. Genome Sequencing and Transcriptomic Analysis

Microalgae cells were harvested 18 h post-yeast inoculation for genome sequencing and transcriptomic analysis. Dialysis tubing cellulose membrane (20 kDa pore size, 76 mm × 49 mm; Sigma-Aldrich, St. Louis, MO, USA) was employed to separate the cultures of *A. platensis* and *S. cerevisiae* before inoculating the *S. cerevisiae* at the beginning of the experiment, as previously described [21]. Total DNA was extracted from *A. platensis* cells using the QIAamp DNA Micro Kit (Qiagen, Redwood, CA, USA) and analyzed using agarose gel electrophoresis to assess DNA integrity and potential RNA/protein contamination. A NanoDrop One spectrophotometer (Thermo Scientific, Waltham, MA, USA) was used to determine DNA purity based on the OD_{260}/OD_{280} ratio, and a Qubit 3.0 fluorometer (Thermo Scientific, Waltham, MA, USA) was used to quantify the DNA concentration. Subsequently, 2.5 µg of qualified DNA was used for library construction, which involved a series of steps, including purification with magnetic beads, fragmentation and end-repair, attachment of barcode labels, pooling of samples, and connection with sequencing adapters. The constructed library was loaded onto the R9.4 sequencing chip and sequenced using a PromethION sequencer (Oxford Nanopore Technologies, Oxford, UK) for 48–72 h. Raw data underwent quality control to remove low-quality and short reads. The high-accuracy Illumina data (Q_{30} > 85%) were assembled using Unicycler 0.4.9 to build a high-quality genome skeleton, which was then combined with Nanopore data to form complete genome maps. Finally, the assembled genome was corrected using Pilon 1.23 to obtain a more accurate genome [22]. Prodigal 2.6.3 was used for protein-coding

gene predictions [23]. tRNA gene prediction was conducted using tRNAscan-SE 2.0 [24]. rRNA gene analysis was conducted using Barrnap 0.7. For genome function annotation, the predicted gene sequences were aligned to GO and KEGG function databases using BLAST. (https://blast.ncbi.nlm.nih.gov/) The circlize R package (version 0.4.12) was used for the circular visualization of genome components and their relationships [25].

Total RNA was extracted from *A. platensis* cells using the QIAamp RNA Mini Kit (Qiagen, CA, USA). The NanoDrop One spectrophotometer was used to determine RNA purity based on the OD_{260}/OD_{280} ratio, and the Agilent 2100 bioanalyzer (Agilent Technologies, CA, USA) was used to determine RNA integrity. Upon quality assessment of the total RNA samples, a cDNA library was constructed using a Maxima Reverse Transcriptase (Thermo Fisher Scientific, MA, USA) prior to sequencing using a sequencing by synthesis (SBS) method on a second-generation high-throughput sequencing platform. Prior to assembly, rigorous read filtering was carried out to ensure data quality. The resulting high-quality clean reads were utilized for de novo transcriptome assembly. CPC2 was used to identify unigenes with coding potential, and BLAST was employed for conduct sequence alignments against the Nr, Nt, SwissProt, KEGG, and GO databases, thereby obtaining annotation information for novel genes.

2.7. qRT-PCR Analysis

Total RNA was isolated from *A. platensis* cells using the TRIzol RNA extractor (Sangon, Shanghai, China) according to the manufacturer's instructions. The quantity and purity of the isolated RNA were analyzed using a Nanodrop ND-1000 spectrophotometer (Thermo Scientific, USA). Then, purified RNA was converted to cDNA using the Maxima Reverse Transcriptase EP0743 (Thermo Scientific, USA). A quantitative real-time PCR assay was performed using the following cycles: 95 °C for 3 min, 45 cycles of 95 °C for 15 s, and 60 °C for 30 s. The 20 µL qRT-PCR reaction mixture comprised 1 µL cDNA, 10 µL Fast qPCR Master Mix, 0.5 µL of each PCR forward/reverse primer, and 8 µL ddH_2O. Melting curve analysis was performed to confirm the purity of the amplification product. All reactions were performed in triplicate, and the Cq values were recorded for each reaction. Gene expression was quantified using the $2^{-\Delta\Delta CT}$ method.

2.8. Statistical Analysis

For each measurement, three independent experiments were conducted to generate a standard deviation. Statistical significance was analyzed using two-way ANOVA or a *t*-test with a multiple comparison Tukey test using the IBM SPSS program (Version 19.0, IBM SPSS, Armonk, NY, USA) and a level of $p < 0.05$.

3. Results and Discussion

3.1. Establishment of the Microalgae–Yeast Co-Culture System

To ensure production quality, commercial microalgae are typically harvested in the late-logarithmic phase, with sufficient biomass yield and relatively short cultivating duration [26]. In the present study, a preharvest culture of *A. platensis* in the late-logarithmic phase was inoculated with *S. cerevisiae* at three yeast-to-microalgae biomass ratios (1:1000, 10:1000, and 100:1000). The co-culture system was then supplemented with 5 g/L of glucose.

According to the kinetics of the OD_{560} and biomass concentration following a co-cultivation duration of 36 h (Figure 1a), the biomass yield in the co-culture was greatly increased by the inoculation of *S. cerevisiae* at yeast-to-microalgae biomass ratios of 1:1000 and 10:1000 ($p < 0.01$), while excess amounts of *S. cerevisiae*, at an inoculation level of 100:1000, appeared to significantly decrease biomass production in the co-culture ($p < 0.05$).

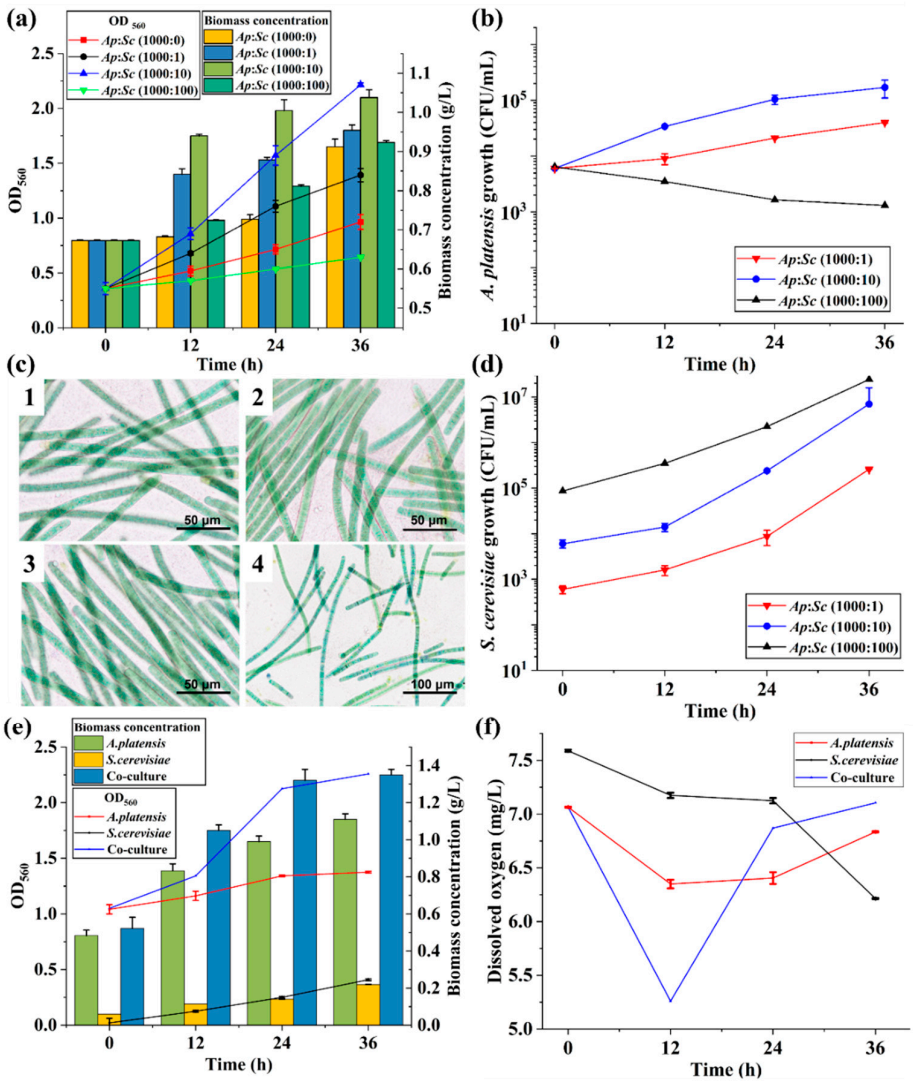


Figure 1. Characterization of *Arthrospira platensis* (*Ap*) and *Saccharomyces cerevisiae* (*Sc*) co-culture systems at different initial inoculation ratios: (**a**) kinetics of OD_{560} and total biomass concentration; (**b**) growth curves of *A. platensis* based on cell counts; (**c**) microscopic morphology of *A. platensis*—(1) monoculture, (2) 1:1000 yeast/microalgae ratio, (3) 10:1000 yeast/microalgae ratio, and (4) 100:1000 yeast/microalgae ratio; (**d**) growth curves of *S. cerevisiae* based on cell counts; (**e**) OD_{560} and biomass concentration kinetics at a yeast/microalgae biomass ratio of 10:1000; (**f**) dissolved oxygen kinetics at a yeast/microalgae biomass ratio of 10:1000.

As shown in Figure 1b, *A. platensis* proliferated throughout the co-cultivation period at inoculation levels of 1:1000 and 10:1000 but gradually died out of the co-culture at an inoculation level of 100:1000. Microscopic observation (Figure 1c) revealed cellular fragmentation of *A. platensis* at the inoculation level of 100:1000, confirming the dying out of *A. platensis* in the presence of excess yeast. Figure 1d illustrates the proliferation of *S. cerevisiae* throughout the co-cultivation period at all three inoculation levels. These results indicate survival stress induced in microalgae by excess yeast, which may explain the significantly lower levels of OD_{560} in the co-culture at an inoculation level of 100:1000 compared to those at lower inoculation levels (Figure 1a). The decline in biomass observed at a 100:1000 ratio was primarily attributed to survival stress in *A. platensis*; however, the underlying mechanisms remain incompletely elucidated due to the paucity of comparative studies.

Based on the above results, a yeast-to-microalgae biomass ratio of 10:1000 was used to establish the preharvest co-culture system for *A. platensis* and *S. cerevisiae*. As shown in Figure 1e, compared to the monocultures of *A. platensis* and *S. cerevisiae*, the co-culture

system had remarkably higher OD_{560} and biomass concentration, indicating excellent biomass yield in the co-culture. As shown in Figure 1f, the level of dissolved oxygen in the *S. cerevisiae* monoculture gradually decreased throughout the 36 h of incubation, correlating with the aerobic catabolism of glucose. The level of dissolved oxygen in the *A. platensis* monoculture sharply decreased within 12 h of incubation and then remained at a constant level before rising gradually after 24 h of incubation, suggesting an increasing contribution of photosynthetic oxygen production after 12 h of incubation because of the exponential growth of microalgae (Figure 1e). In the co-culture system, the level of dissolved oxygen decreased more sharply than in the monocultures within 12 h of incubation. This was followed by a sharp increase over the subsequent 12 h of incubation and then a gradual increase until the end of incubation. This DO pattern was driven by the following metabolic shifts: (1) rapid respiration during the initial phase (0–12 h), fueled by *S. cerevisiae* proliferation under glucose supplementation and phototrophic oxygen release [27]; (2) DO recovery in the subsequent phase (12–24 h), mediated by *A. platensis* as the dominant photoautotroph, with biomass increase (Figure 1e) restoring oxygen production following glucose depletion.

3.2. Color and Compositional Variations in Co-Cultured Microalgae Biomass

Spirulina powders typically exhibit a dark blue–green color and have been reported to have appetite-suppressing properties [28]. However, the appearance of spirulina biomass is not appealing for many food applications. As shown in Figure 2b, *A. platensis* and *S. cerevisiae* in the co-culture can be separated by centrifugation based on their density differences. The lyophilized biomass of co-cultured *A. platensis* exhibited a noticeably lighter green color compared with the biomass observed under monoculture conditions (Figure 2a). This color has been reported to be favorable by consumers from the perspectives of general health interest and environmental concern [29,30]. As revealed by chromatism measurements (Figure 2c), co-cultivation increased the L^* (brightness), $-a$ (green), and $+b$ (yellow) values of the microalgae biomass ($p < 0.05$), confirming the color change from the dark blue–green of the monocultured *A. platensis* to the light green of the co-cultured *A. platensis* (Figure 2a,b). The observed chromatic alteration, concomitant with increased chlorophyll a and carotenoid concentrations (Figure 2d), presumably represents a dilution phenomenon attributable to yeast-derived biomass accumulation or modified pigment organization in the co-cultured microalgae system.

As shown in Figure 2d,e, the co-cultured *A. platensis* had significantly higher levels of chlorophylls and carotenoids than the monocultured microalgae ($p < 0.05$), indicating that co-cultivation with yeast could induce the biosynthesis of chlorophylls and carotenoids. In fact, several previous studies reported the enhancement of microalgae biosynthesis of chlorophylls and carotenoids by co-cultivation with yeast or bacteria. A Chlorella–Saccharomyces co–culture system has been reported to enhance microalgal production of carotenoids [31]. The co-culture of Chlorella and wastewater-borne bacteria has been demonstrated to increase the concentrations of Chl. a, Chl. b, and carotenoids in microalgae biomass [8]. Co-culturing a green alga, *Micractinium* sp. GA001, with the endophytes *Staphylococcus pasteuri* PPE11 and *Yersinia enterocolitica* PPE118 has been shown to significantly increase the total chlorophyll content in microalgae biomass [9].

Figure 2e illustrates the changes in β-carotene and zeaxanthin contents during the in situ light co-cultivation of *A. platensis* and *S. cerevisiae*. Compared with monocultured *A. platensis*, the contents of both carotenoids increased significantly ($p < 0.01$), with β-carotene showing a particularly pronounced increase. As a precursor of terpenoid-derived flavor compounds [32], the increased β-carotene content resulting from co-cultivation may play an important role in enhancing the flavor profile of the microalgae biomass. Similarly,

Figure 2f shows the changes in unsaturated fatty acid (UFA) content. Linoleic acid and γ-linolenic acid, the predominant UFAs in microalgae biomass, were significantly elevated during co-cultivation ($p < 0.05$). These UFAs serve as beneficial components/precursors for volatile flavor compounds through enzymatic or microbial oxidation and cleavage, contributing to the formation of aldehydes, ketones, and alcohols [33,34]. Collectively, the accumulation of these biochemical precursors suggests a synergistic enhancement in flavor-forming potential during co-cultivation.

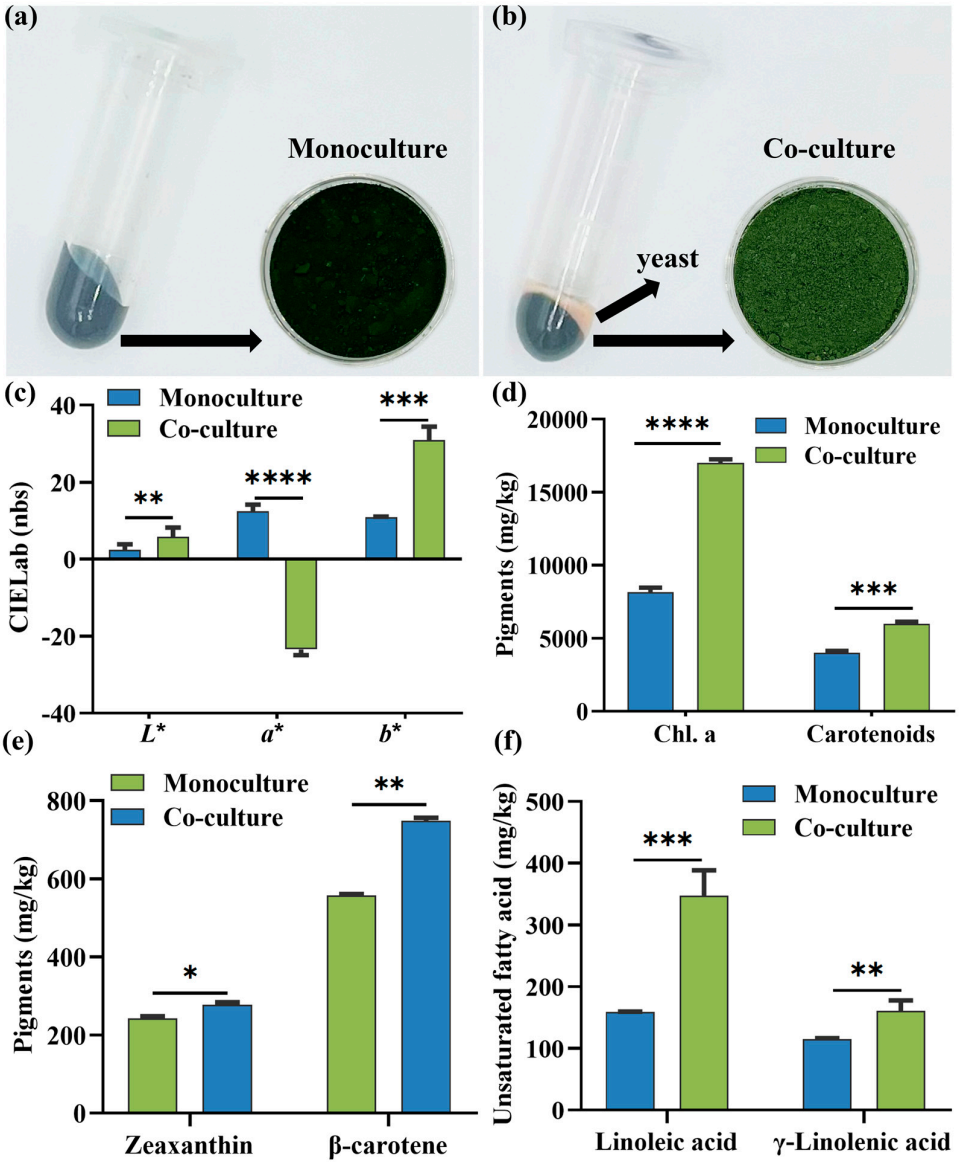


Figure 2. Color and compositional variations in the microalgae biomass of (**a**) monocultured and (**b**) co-cultured *Arthrospira platensis*; (**c**) color difference (ΔE*) measurements; (**d**) chlorophyll a (Chl. a) and carotenoid contents in dry biomass; (**e**) zeaxanthin and β-carotene contents in dry biomass; (**f**) linoleic acid and γ-linolenic acid contents in wet biomass. Asterisks indicate significant differences (**** $p < 0.001$, *** $p < 0.005$, ** $p < 0.01$, and * $p < 0.05$).

3.3. Volatile Flavor Profile of Co-Cultured Microalgae Biomass

Spirulina biomass has some unpleasant odors, such as seaweed and muddy/earthy, which greatly restricts its incorporation into various foods [35]. In the present study, co-cultivation with yeast was found to result in a reduction in the intensity of the unpleasant microalgal odors of "seaweed" and "muddy", as well as to confer pleasant aromas of "floral" and "fruity" to the microalgae biomass (Figure 3a). Conceptually, this is an interesting

finding, as it shows, for the first time, that preharvest co-cultivation with yeast can improve the aroma quality of microalgae biomass.

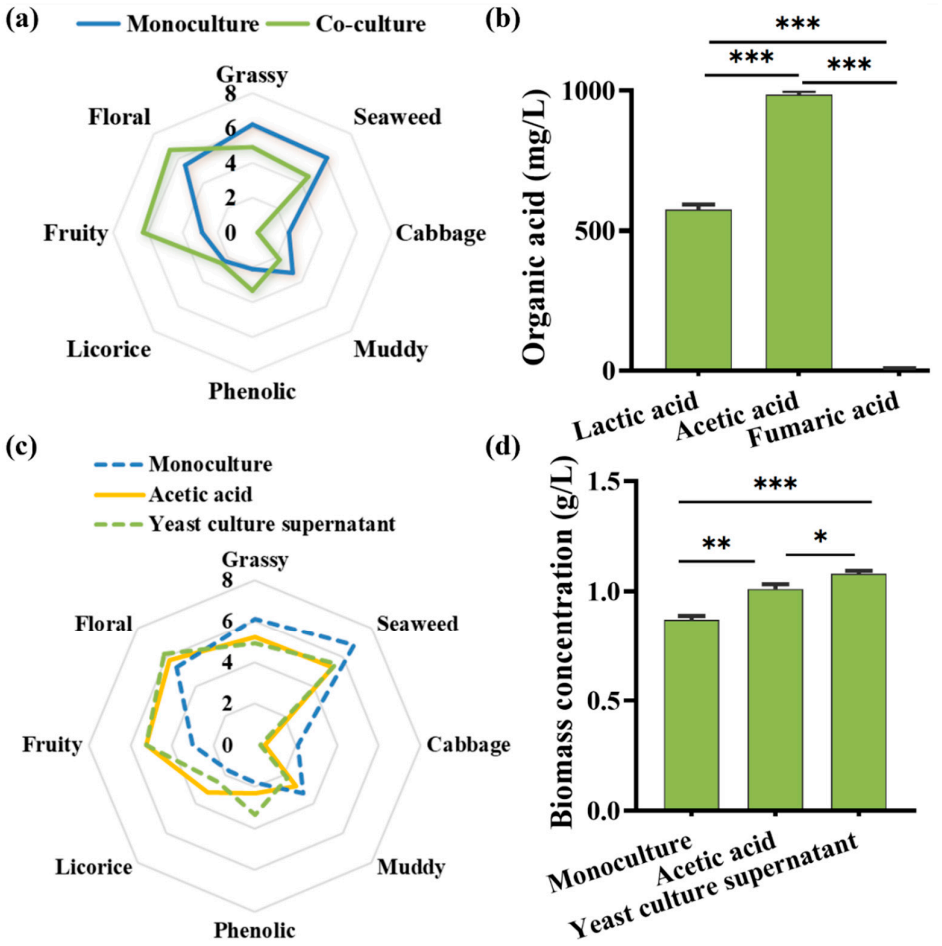


Figure 3. (**a**) Sensory evaluation of lyophilized microalgal biomass based on eight odor attributes; (**b**) composition and concentrations of organic acids in the medium of monocultured *S. cerevisiae*; (**c**) impact of acetic acid supplementation (1.0 g/L) on the aroma quality of lyophilized microalgal biomass; (**d**) impact of acetic acid supplementation (1.0 g/L) on the biomass yield of lyophilized microalgae. Asterisks indicate significant differences (*** $p < 0.005$, ** $p < 0.01$, and * $p < 0.05$).

In the present study, a total of 98 volatile compounds were identified in the monocultured and co-cultured microalgae using SPME-GC-MS, including 29 ketones, 17 aldehydes, 13 alcohols, 8 nitrogenous compounds, 5 phenols, 4 sulfur compounds, 3 organic acids, 2 furans, 1 ester, and 16 hydrocarbons (Table 1). Among them, norisoprenoids (e.g., trans-β-ionone, epoxy-β-ionone, and dihydroactinidiolide) significantly increased in the co-cultured microalgae ($p < 0.05$). Norisoprenoids are a diverse class of aromatic compounds contributing to the floral and fruity nuances of various grapes and wines [36]. Therefore, they might, at least in part, account for the pleasant microalgal aromas of "floral" and "fruity" imparted by co-cultivation with yeast. Notably, quantitative analysis of the OAVs (Table S3) demonstrated that β-ionone, epoxy-β-ionone, (E)-4-oxo-β-ionone, β-cyclocitral, safranal, and dihydroactinidiolide significantly exceeded thresholds, underscoring their dominant role in the enhanced floral and fruity aromas of co-cultured microalgae.

Table 1. Volatile compounds detected in monocultured and co-cultured groups using GC-MS.

Classification	Volatile Compounds	CAS#	LRI	Concentration (μg/kg)	
				Monoculture	Co-Culture
Ketones					
A1	2-Butanone	78–93–3	894	0.305 ± 0.031	0.061 ± 0.002 ***
A2	2,3-Butanedione	431–03–8	971	0.286 ± 0.016	0.352 ± 0.015 *
A3	2-Methyl-3-Heptanone	13,019–20–0	1161	0.489 ± 0.009	10.25 ± 0.204 ***
A4	2-Heptanone	110–43–0	1177	1.82 ± 0.024	2.851 ± 0.042 ***
A5	3-Octanone	106–68–3	1249	0.896 ± 0.005	0.167 ± 0.003 ***
A6	6-Methyl-2-Heptanone	928–68–7	1232	0.285 ± 0.012	0.166 ± 0.003 ***
A7	2-Octanone	111–13–7	1281	1.155 ± 0.028	0.365 ± 0.037 ***
A8	1-Hydroxy-2-Propanone	116–09–6	1292	0.283 ± 0.006	ND
A9	2,2,6-Trimethyl-Cyclohexanone	2408–37–9	1314	0.964 ± 0.008	1.126 ± 0.06 *
A10	6-Methyl-5-Hepten-2-one	110–93–0	1332	1.525 ± 0.029	0.761 ± 0.068 ***
A11	2-Methyl-2-Hepten-4-one	22,319–24–0	1357	0.901 ± 0.015	0.305 ± 0.004 ***
A12	2-Nonanone	821–55–6	1384	2.039 ± 0.008	0.119 ± 0.001 ***
A13	3-Octen-2-one	1669–44–9	1402	ND	0.87 ± 0
A14	2-Decanone	693–54–9	1489	0.591 ± 0.009	0.591 ± 0.001
A15	1-(2-Methyl-1-Cyclopenten-1-yl)-Ethanone	3168–90–9	1589	0.299 ± 0.001	0.241 ± 0.007 ***
A16	4-Hydroxy-4-Methyl-Cyclohexanone	17,429–02–6	1601	25.174 ± 1.775	50.598 ± 0.329 ***
A17	Acetophenone	98–86–2	1648	0.21 ± 0.015	0.167 ± 0.022
A18	3-Acetyl-2-Octanone	27,970–50–9	1663	1.067 ± 0.017	1.744 ± 0.019 ***
A19	2,6,6-Trimethyl-2-Cyclohexene-1,4-Dione	1125–21–9	1691	0.999 ± 0.001	0.576 ± 0.005 ***
A20	1-(4-Methylphenyl)-Ethanone	122–00–9	1775	ND	0.216 ± 0.003
A21	Geranylacetone	3796–70–1	1849	0.807 ± 0.137	1.701 ± 0.04 ***
A22	trans-β-Ionone	79–77–6	1939	11.847 ± 0.125	29.688 ± 0.255 ***
A23	Epoxy-β-Ionone	23,267–57–4	1993	4.212 ± 0.01	13.234 ± 0.191 ***
A24	3,4-Dehydro-β-Ionone	1203–08–3	1999	ND	0.235 ± 0.004
A25	6,10,14-Trimethyl- 2-Pentadecanone	502–69–2	2121	1.017 ± 0.058	3.106 ± 0.077 ***
A26	(E)-4-Oxo-β-Ionone	27,185–77–9	2460	0.136 ± 0.004	0.296 ± 0.003 ***
A27	2-Pyrrolidinone	616–45–5	2027	1.55 ± 0.008	0.467 ± 0.027 ***
A28	Piperitenone Oxide	35,178–55–3	2144	ND	0.647 ± 0.006
A29	3-Ethyl-4-Methyl-1H-Pyrrole-2,5-Dione	20,189–42–8	2251	9.652 ± 0.042	21.381 ± 0.066 ***
Aldehydes					
B1	Acetaldehyde	75–07–0	691	0.293 ± 0.011	0.272 ± 0.018
B2	2-Methyl-Butanal	96–17–3	907	0.812 ± 0.01	0.127 ± 0.005 ***
B3	3-Methyl-Butanal	590–86–3	911	1.3 ± 0.081	0.293 ± 0.05 ***
B4	Pentanal	110–62–3	972	0.41 ± 0.008	1.256 ± 0.045 ***
B5	Hexanal	66–25–1	1075	7.415 ± 0.094	14.336 ± 0.275 ***
B6	Heptanal	111–71–7	1180	0.9 ± 0.008	1.416 ± 0.069 ***
B7	Octanal	124–13–0	1283	ND	0.531 ± 0.009
B8	(E)-2-Heptenal	18,829–55–5	1320	ND	0.199 ± 0
B9	Nonanal	124–19–6	1388	0.622 ± 0.001	3.47 ± 0.22 ***
B10	(E)-2-Octenal	2548–87–0	1425	0.319 ± 0.001	0.601 ± 0.002 ***
B11	3-Furaldehyde	498–60–2	1454	0.117 ± 0.002	0.127 ± 0.002 **
B12	Benzaldehyde	100–52–7	1519	ND	0.127 ± 0.002
B13	(E)-2-Nonenal	18,829–56–6	1533	0.251 ± 0.007	1.04 ± 0.032 ***
B14	β-Cyclocitral	432–25–7	1621	5.31 ± 0.09	5.515 ± 0.004 *
B15	Safranal	116–26–7	1645	0.271 ± 0.009	0.259 ± 0.001
B16	3-Ethyl-Benzaldehyde	34,246–54–3	1707	0.054 ± 0.002	ND
B17	(E, Z)-2,4-Decadienal	25,152–83–4	1810	ND	0.165 ± 0.012
Alcohols					
C1	Ethanol	64–17–5	925	1.854 ± 0.082	0.376 ± 0.011 ***
C2	1-Butanol	71–36–3	1137	12.617 ± 0.177	3.464 ± 0.216 ***
C3	1-Pentanol	71–41–0	1241	1.573 ± 0.006	ND
C4	1-Hexanol	111–27–3	1341	0.763 ± 0.121	0.397 ± 0.064 *
C5	1-Octen-3-ol	3391–86–4	1437	5.504 ± 0.085	4.424 ± 0.101 ***
C6	1-Heptanol	111–70–6	1442	0.442 ± 0.011	ND
C7	2-Ethyl-1-Hexanol	104–76–7	1476	2.418 ± 0.043	4.569 ± 0.767 *
C8	1-Octanol	111–87–5	1544	0.565 ± 0.012	0.147 ± 0.022 ***
C9	1-Nonanol	143–08–8	1646	0.52 ± 0.008	0.164 ± 0.02 ***
C10	Benzyl Alcohol	100–51–6	1862	1.818 ± 0.08	1.357 ± 0.039 ***
C11	Phenylethyl Alcohol	60–12–8	1898	0.196 ± 0.003	0.217 ± 0.011
C12	1-Decanol	112–30–1	1952	ND	0.156 ± 0.003
C13	Phytol	150–86–7	2575	ND	0.259 ± 0.009

Table 1. *Cont.*

Classification	Volatile Compounds	CAS#	LRI	Concentration (μg/kg)	
				Monoculture	Co-Culture
Ketones					
Nitrogenous compounds					
D1	N, N-Dimethyl-Methylamine	75–50–3	642	2.41 ± 0.325	5.367 ± 0.165 ***
D2	Pyrazine	290–37–9	1203	0.09 ± 0.002	ND
D3	2-Methyl-Pyrazine	109–08–0	1259	1.181 ± 0.066	0.162 ± 0.007 ***
D4	2,5-Dimethyl-Pyrazine	123–32–0	1316	1.784 ± 0.005	0.321 ± 0.001 ***
D5	2,6-Dimethyl-Pyrazine	108–50–9	1322	0.298 ± 0.002	ND
D6	2-Ethyl-6-Methyl-Pyrazine	13,925–03–6	1379	0.117 ± 0.003	ND
D7	Pyrrole	109–97–7	1501	0.072 ± 0.01	ND
D8	1-(1H-Pyrrol-2-yl)-Ethanone	1072–83–9	1958	0.078 ± 0.005	0.17 ± 0 ***
Phenols					
E1	3-Methyl-4-Isopropylphenol	3228–02–2	1410	1.258 ± 0.002	0.736 ± 0.013 ***
E2	Butylated Hydroxytoluene	128–37–0	1903	0.057 ± 0.002	0.5 ± 0.016 ***
E3	Phenol	108–95–2	1986	0.204 ± 0.003	15.146 ± 0.012 ***
E4	P-Tert-Butyl-Phenol	98–54–4	2267	0.144 ± 0.001	1.358 ± 0.001 ***
E5	2,4-Di-Tert-Butylphenol	96–76–4	2286	0.369 ± 0.017	1.104 ± 0.078 ***
Sulfur compounds					
F1	Methanethiol	74–93–1	677	0.069 ± 0.008	ND
F2	Dimethyl Disulfide	624–92–0	1063	0.3 ± 0.021	ND
F3	Dimethyl Trisulfide	3658–80–8	1375	0.114 ± 0.005	ND
F4	Dimethyl Sulfoxide	67–68–5	1568	0.069 ± 0	ND
Organic acids					
G1	Acetic Acid	64–19–7	1435	1.319 ± 0.001	0.589 ± 0.001 ***
G2	Octanoic Acid	124–07–2	2037	0.774 ± 0.032	0.408 ± 0.058 ***
G3	n-Decanoic Acid	334–48–5	2248	ND	0.264 ± 0.003
Furans					
H1	3-Methyl-Furan	930–27–8	857	0.102 ± 0.009	0.073 ± 0.005 *
H2	2-Pentyl-Furan	3777–69–3	1224	0.898 ± 0.026	2.368 ± 0.169 ***
Ester					
I1	Dihydroactinidiolide	17,092–92–1	2358	4.982 ± 0.014	16.727 ± 0.223***
Hydrocarbons					
J1	Decane	124–18–5	996	0.84 ± 0.041	0.279 ± 0.001 ***
J2	Undecane	1120–21–4	1089	4.533 ± 0.78	0.284 ± 0.003 ***
J3	1-(1-Cyclohexen-1-yl)-Ethanone	932–66–1	1115	ND	0.221 ± 0.001
J4	5-Ethyldecane	17,302–36–2	1129	0.551 ± 0.025	ND
J5	D-Limonene	5989–27–5	1191	ND	0.078 ± 0.006
J6	Dodecane	112–40–3	1196	12.567 ± 0.079	1.954 ± 0.038 ***
J7	Styrene	100–42–5	1251	1.153 ± 0.027	ND
J8	Tridecane	629–50–5	1297	6.323 ± 0.1	5.507 ± 0.087 ***
J9	2-Methyl-Tridecane	1560–96–9	1353	0.401 ± 0.007	0.409 ± 0.001
J10	3-Methyl-Tridecane	6418–41–3	1363	1.939 ± 0.003	2.193 ± 0.005 ***
J11	Tetradecane	629–59–4	1395	2.979 ± 0.517	5.455 ± 0.118 ***
J12	Pentadecane	629–62–9	1495	49.193 ± 0.109	30.276 ± 5.551 **
J13	Hexadecane	544–76–3	1595	39.117 ± 1.442	24.063 ± 0.051 ***
J14	Heptadecane	629–78–7	1705	421.347 ± 19.469	260.721 ± 4.31 ***
J15	Octadecane	593–45–3	1797	1.331 ± 0.017	ND
J16	(Z)-3-Heptadecene	1,000,141–67–3	1717	36.228 ± 1.801	12.014 ± 0.011 ***

Data are expressed as the mean ± standard deviations (n = 3). ND: not detected; LRI: linear retention index; CAS: Chemical Abstracts Service. The different significance values of $p < 0.05$, $p < 0.01$, and $p < 0.005$ (compared to the monoculture samples) are marked as *, **, and ***.

Cyanobacteria have been found to contain significant amounts of norisoprenoids [37], which are derived from the enzymatic oxidative cleavage of carbon–carbon double bonds in the polyene chains of carotenoids [38], and ionones are a typical class of carotenoid-derived norisoprenoids. In this study, several β-ionone derivatives (e.g., trans-β-ionone, epoxy-β-ionone, 3,4-dehydro-β-ionone, and (E)-4-oxo-β-ionone) were significantly increased in spirulina by co-cultivation with yeast (Table 1). β-Carotene is the flavor precursor of

β-ionone and its derivatives, and its concentration in *A. platensis* was significantly increased by co-cultivation with *S. cerevisiae* (Figure 2e).

The C5–C9 aldehydes deliver desirable fresh–green/fruity to fatty–green/fruity aromas [39]. In the present study, several aldehydes, including pentanal, hexanal, heptanal, (E)-2-heptenal, and octanal, significantly increased in the co-cultured spirulina ($p < 0.05$) (Table 1). These C5–C9 aldehydes should contribute to the microalgal "fruity" aromas endowed by yeast co-cultivation. The odor-active aldehydes are generally derived from the non-enzymatic and enzymatic oxidative degradation of polyunsaturated fatty acids [40]. As mentioned above, co-culturing with *S. cerevisiae* significantly enhanced the accumulation of UFAs in microalgae biomass (Figure 2f), which can increase the flavor precursors for aromatic C5–C9 aldehydes.

Four malodorous volatile organic sulfur compounds (methanethiol, dimethyl disulfide, dimethyl trisulfide, and dimethyl sulfoxide) were identified in the monocultured *A. platensis*. These compounds were not detected in the co-cultured spirulina (Table 1). Cyanobacteria are known to emit alkane thiols (e.g., methanethiol) and methane sulfonic acids (e.g., dimethyl disulfide and dimethyl trisulfide) that have an intense putrid/muddy odor [41]. Co-culturing with *S. cerevisiae* seemed to eliminate these malodorous volatile organic sulfur compounds from the microalgal biomass, leading to a significant reduction in the "muddy" odor of spirulina (Figure 3a).

3.4. Acetic Acid as a Central Effector and Mediator in the Co-Culture System

Boosting the CO_2 fixation efficiency of microalgae under atmospheric conditions is a significant challenge, and several studies have reported that co-cultivation with *S. cerevisiae* can increase the atmospheric growth rate of certain microalgae (e.g., *Chlamydomonas reinhardtii*, *Chlorella pyrenoidosa*, and *Chlorella vulgaris*) [31,42,43]. In general, *S. cerevisiae* is an acidophilic organism that grows better under slightly acidic conditions (pH 4–6); however, the pH of the Zarrouk medium ranged from 9.2 to 11.0, which appears to be adverse to the growth of *S. cerevisiae*. Under alkaline medium conditions, *S. cerevisiae* has been reported to produce negligible ethanol and to fix CO_2 as bicarbonate and organic acids for intracellular pH regulation and medium acidification [44]. In the present study, *S. cerevisiae* grown in 5 g/L of glucose-supplemented Zarrouk medium was found to produce three types of organic acids—acetic acid, lactic acid, and fumaric acid—with acetic acid and lactic acid being predominant (Figure 3b). In the co-culture system, the concentration of acetic acid in the medium increased within 24 h to a maximal level of 0.45 g/L (Figure S1), which is approximately half of that detected in the medium of the monocultured *S. cerevisiae*. Thus, it seems that a significant amount of yeast-derived acetic acid was consumed by *A. platensis* in the co-culture system. The pH of the medium in the co-culture system decreased slightly from 10.49 to 10.32, suggesting that yeast-derived organic acids had a weak impact on the alkaline pH of the Zarrouk medium. In fact, alkaline pH is critical for preventing bacterial contamination during *A. platensis* cultivation. Our co-culture system is, thus, feasible in practical applications from the perspective of maintaining sterile conditions. Although microalgae have been documented to consume acetic acid mixotrophically [45,46], there have been no reports indicating that lactic acid and fumaric acid can also serve as additional sources of organic carbon.

To determine whether yeast-derived acetic acid was responsible for the improved color appearance and aroma quality of co-cultured spirulina, we investigated the effects of medium supplementation with acetic acid and yeast culture supernatant on the growth and volatile flavor profile of *A. platensis*. Acetic acid significantly enhanced microalgal biomass yield and aroma quality ($p < 0.05$), with improvements comparable to those induced by the yeast culture supernatant (Figure 3c,d). Considering that the medium's pH (9.2–11.0)

was not significantly affected by the addition of acetic acid during the cultivation period, acetate seems to be an effector for the yeast-induced changes in color appearance and aroma quality of spirulina (Figure S1).

Genome sequencing and transcriptomic analysis were performed to determine the transcriptional responses of *A. platensis* to yeast co-culture and acetate supplementation. The *A. platensis* FACHB-902 strain used in this study has a single circular chromosome of 6.44 Mb with a total sequence length of 6,437,174 bp and an average G+C content of 44.9%. No plasmid DNA sequences were found (Figure S2). The total RNA extracted from *A. platensis* FACHB-902 exhibited high integrity, and no contamination from *S. cerevisiae* was detected in the simulated co-culture separation (Figure S3). Figure S4 illustrates the relevant KEGG pathways and their corresponding gene counts enriched in the transcriptome of *A. platensis* FACHB-902. Figure 4a specifically illustrates the biosynthetic pathways of flavor precursors (β-carotene, linoleic acid, and γ-linolenic acid), including the fatty acid biosynthesis pathway and the methylerythritol phosphate pathway (MEP pathway). The subsequent cleavage of these precursors generates volatile flavor compounds with floral and fruity aromas (indicated by the boxes in the diagram). The internal control and gene primers for ribulose-1,5-bisphosphate carboxylase/oxygenase (RuBisCO), acetyl-CoA synthetase (ACS), 1-deoxy-D-xylulose 5-phosphate reductase (DXR), 1-deoxy-D-xylulose 5-phosphate synthase (DXS), geranylgeranyl diphosphate synthase (GGPPS), phytoene synthase (PSY), phytoene desaturase (PDS), acetyl-CoA carboxylase (ACCase), fatty acid synthase (FAS), acyl-CoA desaturase (ACD), and delta (6)-fatty-acid desaturase (FAD6) were designed based on the genome and transcripts (Table 2).

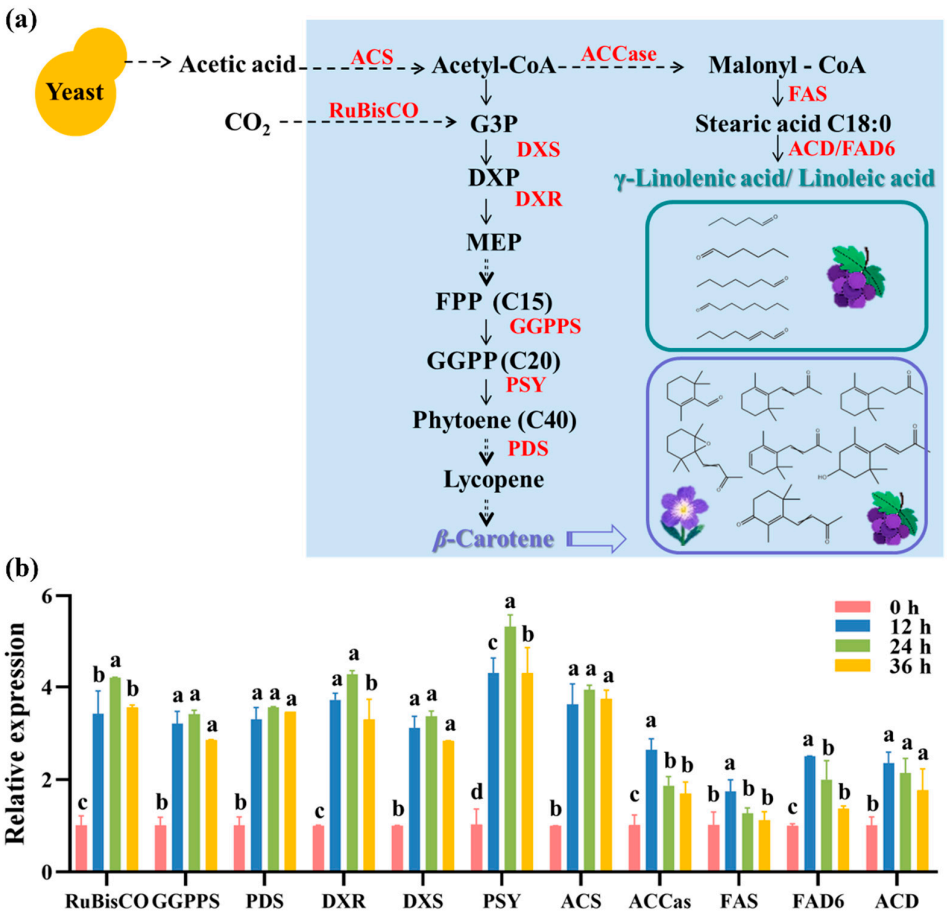


Figure 4. (**a**) Schematic representation of the biosynthesis pathway of beneficial components/flavor precursors (β-carotene, linoleic acid, and γ-linolenic acid) in *A. platensis* and its associated enzymes:

ribulose-1,5-bisphosphate carboxylase/oxygenase (RuBisCO), acetyl-CoA synthetase (ACS), 1-deoxy-D-xylulose 5-phosphate reductase (DXR), 1-deoxy-D-xylulose 5-phosphate synthase (DXS), geranylgeranyl diphosphate synthase (GGPPS), phytoene synthase (PSY), phytoene desaturase (PDS), acetyl-CoA carboxylase (ACCase), fatty acid synthase (FAS), acyl-CoA desaturase (ACD), and delta (6)-fatty acid desaturase (FAD6). Boxes represent volatile flavor compounds (with floral and fruity notes) generated through the cleavage of β-carotene, linoleic acid, and γ-linolenic acid. (**b**) Real-time qPCR analysis of the mRNA expression levels of the genes involved in the biosynthesis of beneficial components/flavor precursors in *A. platensis* during co-cultivation. Different letters above the bars indicate significant differences ($p < 0.05$) for a given enzyme.

Table 2. Primer sequences for real-time quantitative polymerase chain reaction of *A. platensis* FACHB-902.

Genes	Forward and Reverse Primers (5′ → 3′)	
16S (internal control)	*AP* 16S-F	CGTAAACCTCTCCTCAGTTCAG
	AP 16S-F	GAACGGATTCACCGCAGTAT
Ribulose-1,5-bisphosphate carboxylase/oxygenase	RuBisCO-F	TTCTGCTTTGTTGCCTATCCG
	RuBisCO-R	ATCCAAATACGTTACCCACGA
Geranylgeranyl diphosphate synthase	GGPPS-F	ATCTGGAAGCTCAAAAGGCTAC
	GGPPS-R	CGCAACCACCGTTTCCAAA
Phytoene desaturase	PDS-F	AATTATATAGATCCGCTGCAT
	PDS-R	TCTTCACTGACATTATGGGGAC
1-Deoxy-D-xylulose 5-phosphate reductase	DXR-F	AGGCTCATTTTCTCTTTGGTT
	DXR-R	AACACAGAAGTATCCTGCAAC
1-Deoxy-D-xylulose 5-phosphate synthase	DXS-F	CTGTCTCCCCAATATGACCA
	DXS-R	ATTAATACCAGTCACCAGCAT
Phytoene synthase	PSY-F	GCTCTCGGTATTGCTAACCAG
	PSY-R	CCAGCGTTCATCTACTATGCC
Acetyl-CoA synthetase	ACS-F	TCGGTGATCTAATTCTAGCTG
	ACS-R	ATCGCATCAATAAACCCAT
Acetyl-CoA carboxylase	ACCase-F	GGAATGTTAAGCCTCATGCAA
	ACCase-R	CATGGCAAAACTAGCCGTCA
Fatty acid synthase	FAS-F	ATTCGGGGTATTGATCGCCC
	FAS-R	CTCCCCCATGTTCAACGTGA
Acyl-CoA desaturase	ACD-F	TATTTATGGCATTCCTCCACA
	ACD-R	GTAATTCCTAAGCCACCAGT
Delta (6)-fatty-acid desaturase	FAD6-F	GACACCGCTCATTTTCTCGGA
	FAD6-R	ATTCTTCTTTACGCCAGGGTT

F: forward; R: reverse.

In the present study, yeast co-cultivation significantly promoted the expression of genes responsible for the biosynthesis of beneficial components/flavor precursors (β-carotene, linoleic acid, and γ-linolenic acid) in *A. platensis* (Figure 4b). This enhancement coincided with the upregulation of RuBisCO expression over time, indicating that improved photosynthetic performance may underline the increased synthesis of these bioactive compounds.

Acetate has been extensively documented as an effective carbon source for the mixotrophic production of carotenoids and lipids in various microalgae species (e.g., Haematococcus, Chlorella, and Chlamydomonas) [47,48]. As an actively absorbed carbon source for microalgae, acetate is assimilated in the cytosol into acetyl-CoA and subsequently converted in the glyoxysome into succinate via the glyoxylate cycle [49], thereby fueling the tricarboxylic acid (TCA) cycle to enhance gluconeogenesis, fatty acid synthesis, and carotenoid synthesis [50,51]. Acetate assimilation has been shown to promote the biosynthesis of the phytyl side chain of chlorophylls by fueling the TCA cycle and the subsequent glycolytic pathway [52]. Collectively, yeast-derived acetic acid acts as a pivotal metabolic signal and mediator in the inter-organismal information exchange between *A. platensis* and *S. cerevisiae* throughout the co-cultivation process investigated in this study.

4. Conclusions

This study developed an innovative *S. cerevisiae* co-cultivation technique that simultaneously enhanced both the nutritional and sensory qualities of *A. platensis*. At a yeast-to-microalgae ratio of 10:1000, co-culture for 24 h transformed the color of the *A. platensis* biomass from dark blue–green to light green while imparting pleasant floral and fruity aromas. The process significantly increased beneficial components (β-carotene, linoleic acid, and γ-linolenic acid) while effectively eliminating undesirable sulfur compounds. Mechanistic analysis revealed that yeast-derived acetate regulates gene expression in *A. platensis*, promoting the synthesis of these valuable compounds. This preharvest bioprocessing strategy provides an effective solution for overcoming the limitations of *A. platensis* in functional food applications.

Supplementary Materials: The following supporting information can be downloaded at: https://www.mdpi.com/article/10.3390/fermentation11080462/s1, Table S1: Zarrouk medium; Table S2: A6 (Trace elements); Table S3: OAV Values of norisoprenoids. Figure S1: The kinetics of pH and acetic acid in the co-culture system medium; Figure S2: Genome sequencing and transcriptomic analysis of Arthrospira platensis FACHB-902: (a) circular chromosome representation of the A. platensis genome, with circles 1 and 2 (from outside to inside) representing coding sequences transcribed in clockwise and counterclockwise directions, respectively, circles 3 and 4 representing GC content and GC skew, respectively, and circle 5 representing genome sequence information; Figure S3: Agarose gel electrophoresis of the total RNA samples of Arthrospira platensis FACHB-902; Figure S4: Relevant KEGG pathways and the numbers of genes enriched in the transcriptome.

Author Contributions: Conceptualization, Y.Z.; methodology, Y.Z., J.S., Y.C., M.Z. and X.L.; software, Y.Z. and G.F.; validation, Y.Z. and G.F.; formal analysis, Y.Z.; investigation, M.Z.; resources, H.W.; data curation, Y.Z.; writing—original draft preparation, Y.Z.; writing—review and editing, H.W.; visualization, M.Z.; supervision, M.Z.; project administration, H.W.; funding acquisition, H.W. All authors have read and agreed to the published version of the manuscript.

Funding: This research was funded by the Science & Technology Innovation Project of Laoshan Laboratory (grant no. LSKJ2025001003), the Science and Technology Innovation Program of Sanya City (grant no. 2022KJCX59), the Yantai Development Zone Science and Technology Leading Talent Project (grant no. 2021RC014), the Hainan Province's Key Research and Development Project (grant no. ZDYF2024XDNY191), the Major Science and Technology Project of Haikou City (grant no. 2023-001), the Major Scientific and Technological Innovation Project in Shandong Province (grant no. 2022CXGC020414), and the National Natural Science Foundation of China (grant no. 32272240).

Institutional Review Board Statement: Human subjects were employed for sensory evaluation. The study was reviewed and approved by the Ocean University of China IRB (Approval No. OUC-HM-2024-17), and informed consent was obtained from each subject prior to their participation in the study.

Informed Consent Statement: Not applicable.

Data Availability Statement: The original contributions presented in this study are included in the article and Supplementary Materials. Further inquiries can be directed to the corresponding authors.

Conflicts of Interest: The authors declare no conflicts of interest.

References

1. Singh, S.K.; Shukla, L.; Yadav, N.; Singh, P.K.; Singh, S.M.; Yadav, M.K.; Kaushalendra; Kumar, A. Spirulina: From ancient food to innovative super nutrition of the future and its market scenario as a source of nutraceutical. In *Cyanobacterial Biotechnology in the 21st Century*; Springer Nature: Singapore, 2023; pp. 51–61.
2. Subashchandrabose, S.R.; Ramakrishnan, B.; Megharaj, M.; Venkateswarlu, K.; Naidu, R. Consortia of cyanobacteria/microalgae and bacteria: Biotechnological potential. *Biotechnol. Adv.* **2011**, *29*, 896–907. [CrossRef] [PubMed]

3. Padmaperuma, G.; Kapoore, R.V.; Gilmour, D.J.; Vaidyanathan, S. Microbial consortia: A critical look at microalgae co-cultures for enhanced biomanufacturing. *Crit. Rev. Biotechnol.* **2018**, *38*, 690–703. [CrossRef] [PubMed]
4. Pandey, J.P.; Pathak, N.; Tiwari, A.S. Standardization of pH and light intensity for the biomass production of *Spirulina platensis*. *J. Algal Biomass Util.* **2010**, *1*, 93–102.
5. Naidoo, R.K.; Simpson, Z.F.; Oosthuizen, J.R.; Bauer, F.F. Nutrient exchange of carbon and nitrogen promotes the formation of stable mutualisms between *Chlorella sorokiniana* and *Saccharomyces cerevisiae*: Under engineered synthetic growth conditions. *Front. Microbiol.* **2019**, *10*, 00609. [CrossRef]
6. Shu, C.H.; Tsai, C.C.; Chen, K.Y.; Liao, W.H.; Huang, H.C. Enhancing high quality oil accumulation and carbon dioxide fixation by a mixed culture of Chlorella sp. and *Saccharomyces cerevisiae*. *J. Taiwan Inst. Chem. Eng.* **2013**, *44*, 936–942. [CrossRef]
7. Naseema Rasheed, R.; Pourbakhtiar, A.; Mehdizadeh Allaf, M.; Baharlooeian, M.; Rafiei, N.; Alishah Aratboni, H.; Morones-Ramírez, J.R.; Winck, F.V. Microalgal co-cultivation-recent methods, trends in omic-studies, applications, and future challenges. *Front. Bioeng. Biotechnol.* **2023**, *11*, 1193424. [CrossRef]
8. Huo, S.; Kong, M.; Zhu, F.; Qian, J.; Huang, D.; Chen, P.; Ruan, R. Co-culture of Chlorella and wastewater-borne bacteria in vinegar production wastewater: Enhancement of nutrients removal and influence of algal biomass generation. *Algal Res.* **2020**, *45*, 101744. [CrossRef]
9. Sonowal, S.; Palani, N.P.; Ahmed, R.; Debbarma, J.; Chikkaputtaiah, C.; Basar, E.; Velmurugan, N. Himalayan bacterial endophytes enhance microalgal cell numbers and chlorophyll content in synthetic co-culture. *J. Appl. Phycol.* **2022**, *34*, 2383–2400. [CrossRef]
10. da Silva Vaz, B.; Costa, J.A.; de Morais, M.G. CO_2 Biofixation by the Cyanobacterium *Spirulina* sp. LEB 18 and the Green Alga *Chlorella fusca* LEB 111 Grown using gas effluents and solid residues of thermoelectric origin. *Appl. Biochem. Biotechnol.* **2016**, *178*, 418–429. [CrossRef]
11. Harvath, P.; Reidy, S.; Byer, J. Identification of organic acids in used engine oil residues by pyrolysis-comprehensive 2D gas chromatography-time of flight mass spectrometry. *SAE Mobilus* **2016**, *1*, 2274.
12. Wellburn, A.R. The spectral determination of Chlorophylls a and b, as well as total carotenoids, using various solvents with spectrophotometers of different resolution. *J. Plant Physiol.* **1994**, *144*, 307–313. [CrossRef]
13. Chen, J.; Zhang, R.; Zhang, G.; Liu, Z.; Jiang, H.; Mao, X. Heterologous expression of the plant-derived astaxanthin biosynthesis pathway in *Yarrowia lipolytica* for glycosylated astaxanthin production. *J. Agric. Food Chem.* **2023**, *71*, 2943–2951. [CrossRef]
14. *ISO 8589*; Sensory Analysis. General Guidance for the Design of Test Rooms. International Organization for Standardization: Geneva, Switzerland, 2007.
15. Li, X.; Xie, W.; Bai, F.; Wang, J.; Zhou, X.; Gao, R.; Xu, X.; Zhao, Y. Influence of thermal processing on flavor and sensory profile of sturgeon meat. *Food Chem.* **2022**, *374*, 131689. [CrossRef]
16. Qian, S.; Liu, K.; Wang, J.; Bai, F.; Gao, R.; Zeng, M.; Wu, J.; Zhao, Y.; Xu, X. Capturing the impact of oral processing behavior and bolus formation on the dynamic sensory perception and composition of steamed sturgeon meat. *Food Chem. X* **2023**, *17*, 100553. [CrossRef]
17. *ISO 5496:1984*; Sensory Analysis—Methodology—Initiation and Training of Assessors in the Detection and Recognition of Odours. International Organization for Standardization (ISO): Geneva, Switzerland, 1984.
18. *ISO 8586:2012*; Sensory Analysis—General Guidance for the Selection, Training and Monitoring of Selected Assessors and Expert Sensory Assessors. International Organization for Standardization (ISO): Geneva, Switzerland, 2012.
19. *GB/T 39625*; Sensory Analysis—Methodology—General Guidance for Establishing a Sensory Profile. Standardization Administration of China: Beijing, China, 2020.
20. Zhao, Y.; Wang, Y.; Li, C.; Li, L.; Yang, X.; Wu, Y.; Chen, S.; Zhao, Y. Novel insight into physicochemical and flavor formation in naturally fermented tilapia sausage based on microbial metabolic network. *Food Res. Int.* **2021**, *141*, 110122. [CrossRef] [PubMed]
21. Song, H.; Lavoie, M.; Fan, X.; Tan, H.; Liu, G.; Xu, P.; Fu, Z.; Paerl, H.W.; Qian, H. Allelopathic interactions of linoleic acid and nitric oxide increase the competitive ability of Microcystis aeruginosa. *ISME J.* **2017**, *11*, 1865–1876. [CrossRef]
22. Wick, R.R.; Judd, L.M.; Gorrie, C.L.; Holt, K.E. Unicycler: Resolving bacterial genome assemblies from short and long sequencing reads. *PLoS Comput. Biol.* **2016**, *13*, e1005595. [CrossRef] [PubMed]
23. Hyatt, D.; Chen, G.-L.; LoCascio, P.F.; Land, M.L.; Larimer, F.W.; Hauser, L.J. Prodigal: Prokaryotic gene recognition and translation initiation site identification. *BMC Bioinform.* **2010**, *11*, 119. [CrossRef] [PubMed]
24. Chan, P.P.; Lin, B.Y.; Mak, A.J.; Lowe, T.M. tRNAscan-SE 2.0: Improved detection and functional classification of transfer RNA genes. *Nucleic Acids Res.* **2021**, *49*, 9077–9096. [CrossRef]
25. Gu, Z.; Gu, L.; Eils, R.; Schlesner, M.; Brors, B. circlize implements and enhances circular visualization in R. *Bioinformatics* **2014**, *30*, 2811–2812. [CrossRef]
26. Sui, Y.; Jiang, Y.; Moretti, M.; Vlaeminck, S.E. Harvesting time and biomass composition affect the economics of microalgae production. *J. Clean. Prod.* **2020**, *259*, 120782. [CrossRef]
27. Strohm, J.; Dale, R. Dissolved Oxygen Measurement in Yeast Propagation. *Ind. Eng. Chem.* **1961**, *53*, 760–764. [CrossRef]

28. Schlintl, C.; Schienle, A. Effects of coloring food images on the propensity to eat: A placebo approach with color suggestions. *Front. Psychol.* **2020**, *11*, 589826. [CrossRef]
29. Van der Stricht, H.; Profeta, A.; Hung, Y.; Verbeke, W. Consumers' willingness-to-buy pasta with microalgae proteins–Which label can promote sales? *Food Qual. Prefer.* **2023**, *110*, 104948. [CrossRef]
30. Hutchings, J.B. *Food Colour and Appearance in Perspective. Food Colour and Appearance*; Springer: Boston, MA, USA, 1994; pp. 1–29.
31. Xu, Z.; Theodoropoulos, C.; Pittman, J.K. Optimization of a Chlorella–Saccharomyces co–culture system for enhanced metabolite productivity. *Algal Res.* **2024**, *79*, 103455. [CrossRef]
32. da Silva Souza, M.A.; Peres, L.E.; Peres, L.E.; Freschi, J.R.; Purgatto, E.; Lajolo, F.M.; Hassimotto, N.M. Changes in flavonoid and carotenoid profiles alter volatile organic compounds in purple and orange cherry tomatoes obtained by allele introgression. *J. Sci. Food Agric.* **2020**, *100*, 1662–1670. [CrossRef] [PubMed]
33. Duan, S.; Tian, Z.; Zheng, X.; Tang, X.; Li, W.; Huang, X. Characterization of flavour components and identification of lipid flavour precursors in different cuts of pork by phospholipidomics. *Food Chem.* **2024**, *458*, 139422. [CrossRef]
34. Li, X.; Qi, L.; Zang, N.; Zhao, L.; Sun, Y.; Huang, X.; Wang, H.; Yin, Z.; Wang, A. Integrated metabolome and transcriptome analysis of the regulatory network of volatile ester formation during fruit ripening in pear. *Plant Physiol. Biochem.* **2022**, *185*, 80–90. [CrossRef] [PubMed]
35. Colonia, B.S.O.; de Melo Pereira, G.V.; Carvalho, J.C.d.; Karp, S.G.; Rodrigues, C.; Soccol, V.T.; Fanka, L.S.; Soccol, C.R. Deodorization of algae biomass to overcome off-flavors and odor issues for developing new food products: Innovations, trends, and applications. *Food Chem. Adv.* **2023**, *2*, 100270. [CrossRef]
36. Mele, M.A.; Kang, H.-M.; Lee, Y.T.; Islam, M.Z. Grape terpenoids: Flavor importance, genetic regulation, and future potential. *Crit. Rev. Food Sci. Nutr.* **2020**, *61*, 1429–1447. [CrossRef]
37. Milovanović, I.; Mišan, A.; Simeunović, J.; Kovač, D.; Jambrec, D.; Mandić, A. Determination of volatile organic compounds in selected strains of cyanobacteria. *J. Chem.* **2015**, *2015*, 969542. [CrossRef]
38. Ahrazem, O.; Gómez-Gómez, L.; Rodrigo, M.J.; Avalos, J.; Limón, M.C. Carotenoid cleavage oxygenases from microbes and photosynthetic organisms: Features and functions. *Int. J. Mol. Sci.* **2016**, *17*, 1781. [CrossRef] [PubMed]
39. Garcia-Oliveira, P.; Jimenez-Lopez, C.; Lourenço-Lopes, C.; Chamorro, F.; Pereira, A.G.; Carrera-Casais, A.; Fraga-Corral, M.; Carpena, M.; Simal-Gandara, J.; Prieto, M.A. Evolution of flavors in extra virgin olive oil shelf-life. *Antioxidants* **2021**, *10*, 368. [CrossRef] [PubMed]
40. Liang, X.; Qian, R.; Wang, D.; Liu, L.; Sun, C.; Lin, X. Lipid-Derived Aldehydes: New Key Mediators of plant growth and stress responses. *Biology* **2022**, *11*, 1590. [CrossRef] [PubMed]
41. Achyuthan, K.E.; Harper, J.C.; Manginell, R.P.; Moorman, M.W. Volatile metabolites emission by in vivo microalgae—An overlooked opportunity? *Metabolites* **2017**, *7*, 39. [CrossRef]
42. Karitani, Y.; Yamada, R.; Matsumoto, T.; Ogino, H. Improvement of cell growth in green algae *Chlamydomonas reinhardtii* through co-cultivation with yeast *Saccharomyces cerevisiae*. *Biotechnol. Lett.* **2024**, *46*, 431–441. [CrossRef]
43. La, A.; Perré, P.; Taidi, B. Process for symbiotic culture of *Saccharomyces cerevisiae* and *Chlorella vulgaris* for in situ CO_2 mitigation. *Appl. Microbiol. Biotechnol.* **2019**, *103*, 731–745. [CrossRef]
44. Peña, A.; Sánchez, N.S.; Álvarez, H.; Calahorra, M.; Ramírez, J. Effects of high medium pH on growth, metabolism and transport in *Saccharomyces cerevisiae*. *FEMS Yeast Res.* **2015**, *15*, 25673753. [CrossRef]
45. Arora, N.; Patel, A.; Mehtani, J.; Pruthi, P.A.; Pruthi, V.; Poluri, K.M. Co-culturing of oleaginous microalgae and yeast: Paradigm shift towards enhanced lipid productivity. *Environ. Sci. Pollut. Res.* **2019**, *26*, 16952–16973. [CrossRef]
46. Proietti Tocca, G.; Agostino, V.; Menin, B.; Tommasi, T.; Fino, D.; Di Caprio, F. Mixotrophic and heterotrophic growth of microalgae using acetate from different production processes. *Rev. Environ. Sci. Bio/Technol.* **2024**, *23*, 93–132. [CrossRef]
47. Liaqat, F.; Khazi, M.I.; Bahadar, A.; He, L.; Aslam, A.; Liaquat, R.; Agathos, S.N.; Li, J. Mixotrophic cultivation of microalgae for carotenoid production. *Rev. Aquac.* **2023**, *15*, 35–61. [CrossRef]
48. Ma, X.; Mi, Y.; Zhao, C.; Wei, Q. A comprehensive review on carbon source effect of microalgae lipid accumulation for biofuel production. *Sci. Total Environ.* **2022**, *806*, 151387. [CrossRef]
49. De Bellis, L.; Luvisi, A.; Alpi, A. Aconitase: To be or not to be inside plant glyoxysomes, that is the question. *Biology* **2020**, *9*, 162. [CrossRef]
50. Kong, F.; Romero, I.T.; Warakanont, J.; Li-Beisson, Y. Lipid catabolism in microalgae. *New Phytol.* **2018**, *218*, 1340–1348. [CrossRef] [PubMed]

51. Raita, S.; Feldmane, L.; Kusnere, Z.; Spalvins, K.; Kuzmika, I.; Berzina, I.; Mika, T. Microbial carotenoids production: Strains, conditions, and yield affecting factors. *Environ. Clim. Technol.* **2023**, *27*, 1027–1048. [CrossRef]
52. Nabeta, K.; Saitoh, T.; Adachi, K.; Komuro, K. Biosynthesis of phytyl side-chain of Chlorophyll a: Apparent reutilization of carbon dioxide evolved during acetate assimilation in biosynthesis of chloroplastidic isoprenoid. *Chem. Commun.* **1998**, *29*, 671–672. [CrossRef]

Disclaimer/Publisher's Note: The statements, opinions and data contained in all publications are solely those of the individual author(s) and contributor(s) and not of MDPI and/or the editor(s). MDPI and/or the editor(s) disclaim responsibility for any injury to people or property resulting from any ideas, methods, instructions or products referred to in the content.